Periodica Polytechnica Civil Engineering, 69(4), pp. 1078–1091, 2025

Automated Graph Theoretic Force Method and its Application in Optimal Design of Frame Structures

Ali Kaveh[1]*, Neda Khavaninzadeh[1]

[1] School of Civil Engineering, Iran University of Science and Technology, P. O. B. 16765-163, Narmak, 16846-13114 Tehran, Iran
* Corresponding author, e-mail: alikaveh@iust.ac.ir

Received: 12 May 2025, Accepted: 28 August 2025, Published online: 05 September 2025

Abstract

In this study, the graph-theoretic force method is applied to the optimal design of frame structures and systematically compared with the conventional displacement method. The optimization is performed using the Water Strider Algorithm (WSA), a recently developed bio-inspired metaheuristic, whose population-based search strategy is integrated with both analysis approaches. To ensure reproducibility, all key WSA parameters are reported, and large-scale highly indeterminate frame examples (up to 292 members) are tested, extending beyond previous benchmark studies. In addition, a counterexample with DKI < DSI is included, demonstrating that the relative efficiency of the two methods is problem-dependent rather than universal. The results show that for large-scale highly indeterminate frames, the graph-theoretic force method combined with WSA significantly reduces computational time while maintaining accuracy comparable to the displacement method. These findings highlight both the scalability and the limitations of the graph-theoretic force method, offering a balanced perspective for its practical application in structural optimization.

Keywords

force (flexibility) method, displacement (stiffness) method, tall buildings, Degree of Static Indeterminacy (DSI), Degree of Kinematic Indeterminacy (DKI)

1 Introduction

Two methods of structural analysis are force method and displacement method. The force method structural analysis is not fully developed compared to the displacement method due to its difficulty in generating sparse flexibility matrices. Thus, the advantages of the force method in nonlinear analysis and optimization have been neglected [1].

One of the criterions for choosing the method of structural analysis is the comparison of their DSI and DKI. If the DSI value is lower, it will be beneficial to use the force method, and if the DKI value is lower, the use of the displacement method is recommended [2].

In previous study, Kaveh and Zaerreza [3], the graph-theoretic force method was combined with the improved particle swarm optimization (PSO-SRM) and applied to benchmark-scale frame structures. While these works demonstrated the efficiency of the force method compared to the displacement approach, the optimization was limited to relatively small or medium-sized structures and was focused mainly on algorithmic development. In contrast, the present study introduces the Water Strider Algorithm (WSA), a recent bio-inspired metaheuristic, into the optimal design of frame structures using the graph-theoretic force method. The novelty of this research lies in

1. employing a fundamentally different optimizer with distinct search mechanisms compared to PSO-based methods, and
2. extending the analysis to large-scale, highly indeterminate high-rise frames (with up to 292 members).

This combination highlights the scalability and practical applicability of the graph-theoretic force method when integrated with the modern metaheuristic algorithms. The overall research process is shown in the flowchart in Fig. 1.

2 Force method

In this article, examples of some special high-rise frames are optimized, which are analyzed by the force method and displacement approach. The selected structures have less DSI than DKI, and therefore the reduction of analysis time and memory saving in the force method is expected.

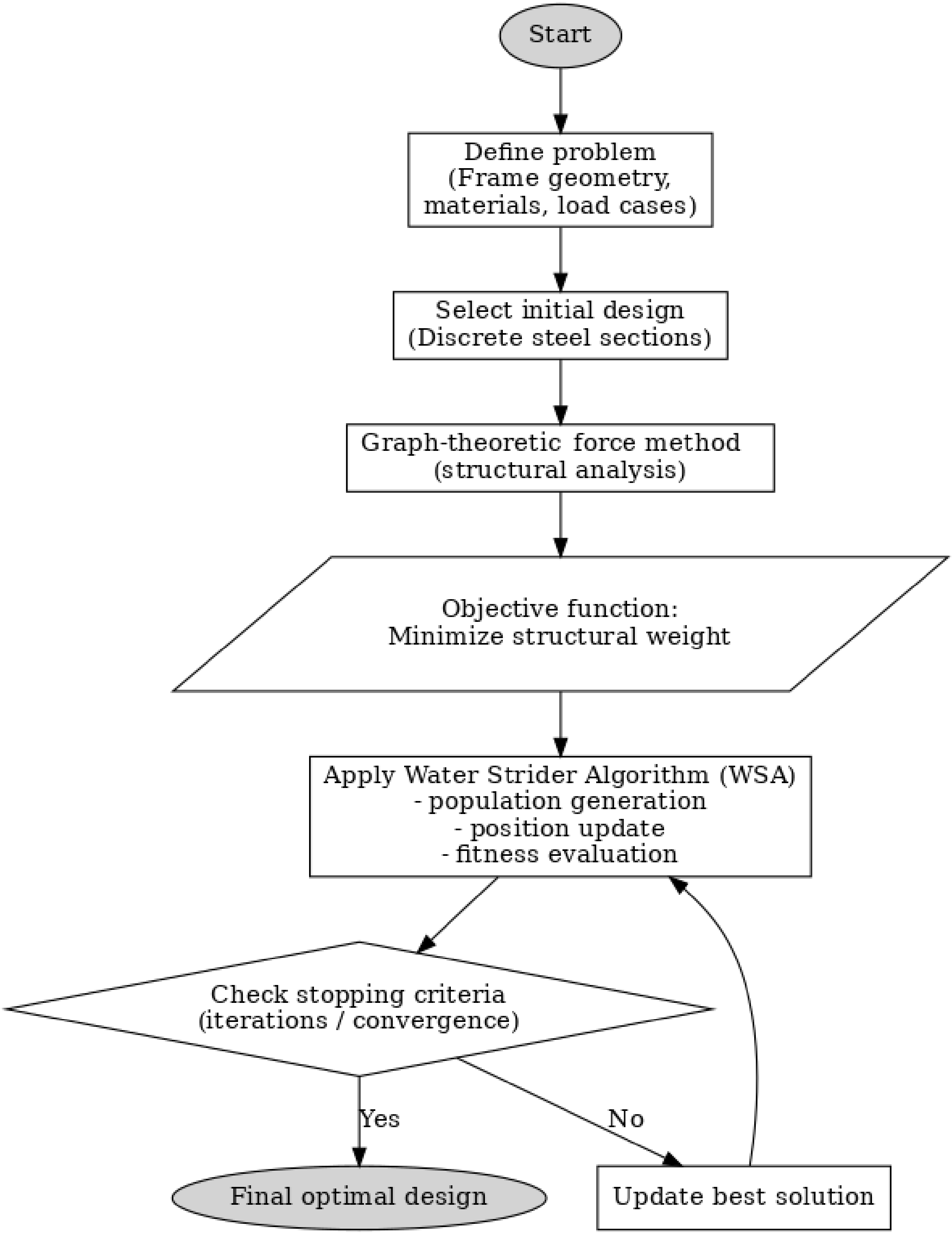

Fig. 1 Flowchart presenting the methodology

In the force method used for structural analysis, member forces are used as unknowns. This method is attractive to engineers because the properties of the members of a structure often depend on member forces rather than joint displacements.

Force method has been extensively utilized until the 1960s, Argyris and Kelsey [4]. However, following the developments of digital computers and the convenience associated with the transfer method, it garnered significant attention from researchers. Consequently, the force method, along with some of its benefits, has been overlooked in the contexts of nonlinear analysis and optimization, Kaveh [5].

Topological force methods are developed by de C. Henderson [6]; Maunder [7]; and de Henderson and Maunder [8]. Algebraic force methods have been developed by Denke [9]; Robinson and Haggenmacher [10]; Topcu [11]; Kaneko et al. [12]; and Soyer and Topcu [13]. The later methods are simple; however, the corresponding algorithms act like black boxes and no suitable interpretation can be provided.

Following the above mentioned topological methods, Kaveh [14–16] proposed graph-based methods for analyzing frame structures. These corresponding approaches have been broadened to encompass a diverse range of skeletal frameworks, including rigidly connected frames, pin-connected planar trusses, and ball-jointed spatial trusses [17, 18].

The simultaneous analysis and design utilizing the force method has been explored in the studies conducted by Kaveh and Rahami [19], as well as by Kaveh and Malakouti Rad [20]. Additionally, the application of finite element analysis through the graph-theoretic force method is detailed in the research of Kaveh et al. [21].

2.1 Formulation of force method

The stress distribution $\boldsymbol{r}$ caused by load $\boldsymbol{p}$ and redundant $\boldsymbol{q}$ in members for linear analysis with force method can be written as follows:

$$\boldsymbol{r} = \boldsymbol{B}_0 \boldsymbol{p} + \boldsymbol{B}_1 \boldsymbol{q}. \quad (1)$$

This formula shows that the internal forces of the structure are a function of the applied forces and the redundant. Where $\boldsymbol{B}_0$ and $\boldsymbol{B}_1$ are the matrices that will be examined in the following. $\boldsymbol{B}_0\boldsymbol{p}$ is known as a specific solution that satisfies the equilibrium with the imposed load, and $\boldsymbol{B}_1\boldsymbol{q}$ is a complementary solution consisting of a maximum set of independent self-equilibrium stress systems (S.E.Ss) known as the static basis.

The stress resultant in a structure can be obtained as

$$\boldsymbol{r} = \left[\boldsymbol{B}_0 - \boldsymbol{B}_1 \left(\boldsymbol{B}_1^t \boldsymbol{F}_m \boldsymbol{B}_1 \right)^{-1} \left(\boldsymbol{B}_1^t \boldsymbol{F}_m \boldsymbol{B}_0 \right) \right] \boldsymbol{p}. \quad (2)$$

In this context, the matrix $\boldsymbol{G} = \boldsymbol{B}_1^t \boldsymbol{F}_m \boldsymbol{B}_1$ represents the flexibility matrix of the structure, where $\boldsymbol{F}_m$ denotes the unassembled flexibility matrix. To ensure the efficiency of the force method [1, 2], the matrix $\boldsymbol{G}$ must meet the following criteria:

1. It should be **sparse**, meaning that it contains a high proportion of zero elements, which helps reduce computational complexity.
2. It needs to be **well-conditioned**, ensuring numerical stability and reliability in calculations.
3. It must be **well-structured**, specifically being narrowly banded, which enhances the efficiency of matrix operations.

2.2 Formation of $\boldsymbol{B}_0$ and $\boldsymbol{B}_1$ matrices

Columns $\boldsymbol{B}_1$ form the static basis of S. Consider a simple frame as shown in Fig. 2 (a).

The cycles shown in Fig. 2 (b) are fundamental cycles. These cycles are independent, but due to the length of the cycles, we do not form our self-balanced systems on these. Instead, we form them on a cycle basis. They are shown in Fig. 2 (c). These are also independent but shorter. So, the values of matrix $\boldsymbol{B}_1$ will decrease [22].

To generate the entries of the $\boldsymbol{B}_0$ matrix, a primary structure S should be chosen. Then a spanning forest is formed including all the ground nodes of S.

Fig. 3 shows the structure of S and the covering forest. Through these two trees, the forces on the nodes are transferred efficiently to the ground.

$\boldsymbol{B}_0$ is a $3M(S) \times 3NL(S)$ matrix, with $M(S)$ and $NL(S)$ being the number of members and loaded nodes of S, respectively. If all free nodes are loaded, $NL(S) = N(S) - NG(S)$ where $NG(S)$ is the number of support nodes.

The matrix $\boldsymbol{B}_0$ can be obtained by assembling the submatrices $[\boldsymbol{B}_0]_{ij}$. Its schematic form is given in Fig. 4.

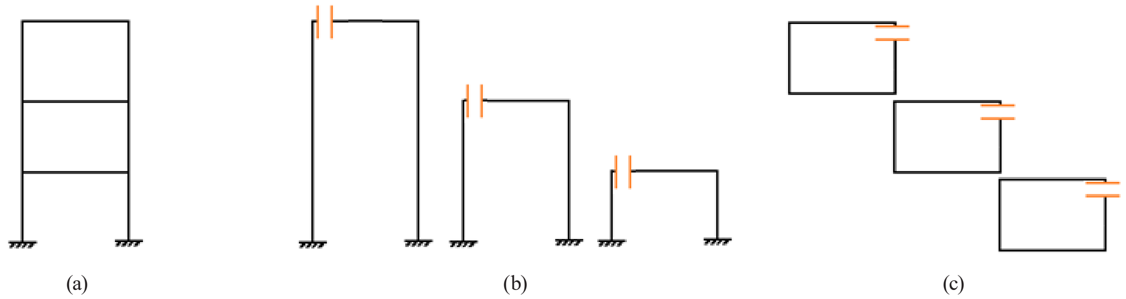

Fig. 2 A simple frame with different cycle bases: (a) a simple frame, (b) fundamental cycle basis, (c) localized cycle basis

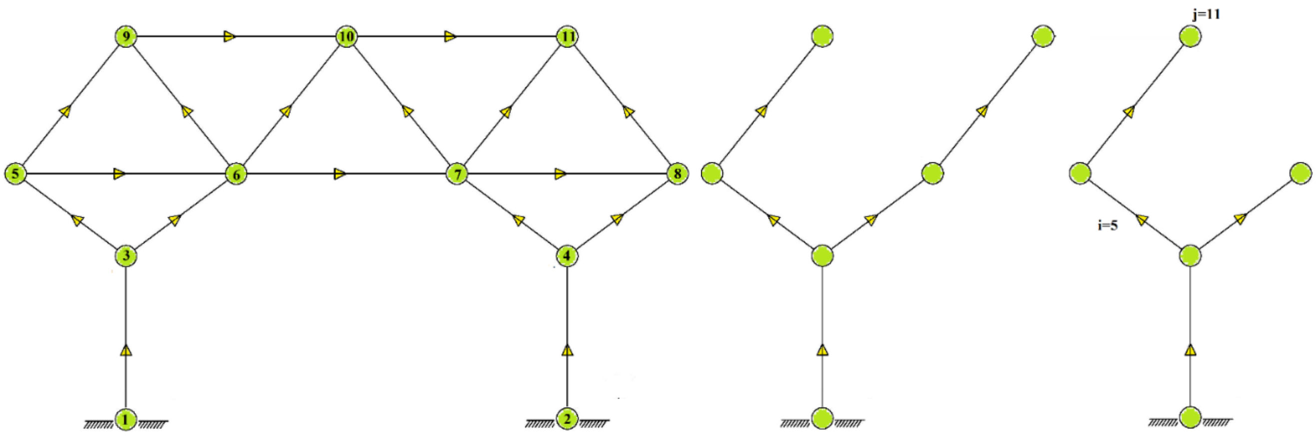

Fig. 3 The structure of S and the covering forest

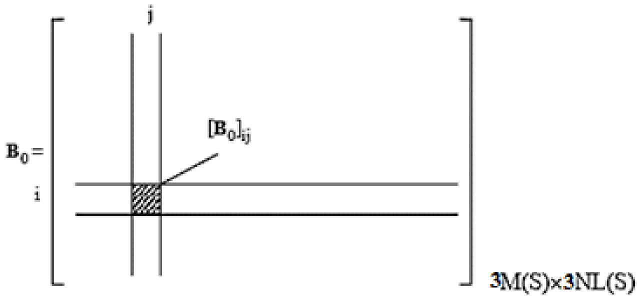

Fig. 4 Schematic of the $\boldsymbol{B}_0$ matrix

$[\boldsymbol{B}_0]_{ij}$ for member i and node j is given by a 3 × 3 submatrix as

$$[\boldsymbol{B}_0]_{ij} = \alpha_{ij} \begin{bmatrix} \cos\alpha & \sin\alpha & 0 \\ -\Delta y & \Delta x & 1 \\ \varepsilon L \sin\alpha & \varepsilon L \cos\alpha & -1 \end{bmatrix}. \quad (3)$$

In this context, Δx, Δy represent the differences in the coordinates of node j relative to the lower numbered end of member i within the chosen global coordinate system. The α is the angle of the member i with the coordinate system. The orientation coefficient α_{ij} is defined as follows:

$$\alpha_{ij} = \begin{cases} +1 & \text{if member is positively oriented in the tree containing node } j \\ -1 & \text{if member is negatively oriented in the tree containing node } j \\ 0 & \text{if member is not in the tree containing node } j \end{cases}.$$

The matrix $\boldsymbol{B}_1$ is a $3M(S) \times 3b_1(S)$ matrix that is constructed using the elements from a chosen cycle. $M(S)$ is the number of members and $b_1(S)$ is the first Betti number. In the case of a spatial structure, each cycle can generate six self-equilibrium stress systems, while for a two-dimensional structure, three self-equilibrium stress systems can be derived.

Let us consider a specific cycle, denoted as C_j, along with a member belonging to this cycle, which we will refer to as its generator. To analyze this member effectively, it is cut near its initial node. At this juncture, six components are applied, as illustrated in Fig. 5. Each of these components represents the forces and moments acting on the node, facilitating the derivation of the stress systems used to construct the matrix $\boldsymbol{B}_1$.

This process enables the representation of the relationship between the loads and the resulting stresses within the cycle, contributing to the overall analysis and design of the structure.

It is like a tree if we enter the force in j and at the end of the element i is found in the reactions.

The matrix $\boldsymbol{B}_1$ can be obtained by assembling the submatrices $[\boldsymbol{B}_1]_{ij}$ as shown in Fig. 6.

$[\boldsymbol{B}_1]_{ij}$ for the member i and node j is given by a 3 × 3 submatrix as

$$[\boldsymbol{B}_1]_{ij} = \beta_{ij} \begin{bmatrix} \cos\alpha & \sin\alpha & 0 \\ -\Delta y & \Delta x & 1 \\ \varepsilon L \sin\alpha & \varepsilon L \cos\alpha & -1 \end{bmatrix} \quad (4)$$

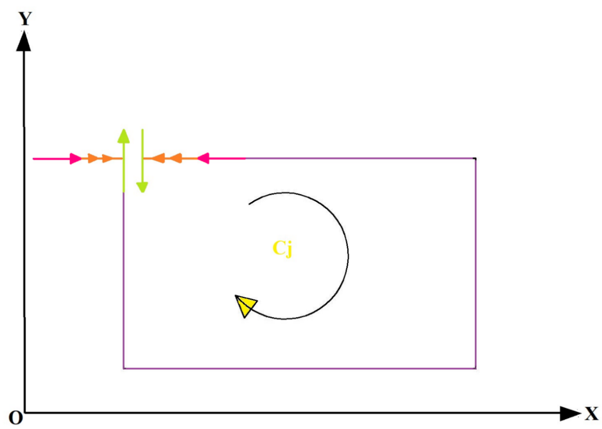

Fig. 5 A cycle and self-equilibrium stress systems

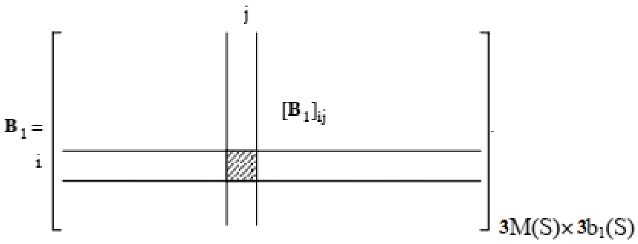

Fig. 6 Schematic of the $\boldsymbol{B}_1$ matrix

$$\beta_{ij} = \begin{cases} +1 & \text{if member has same oriented of the cycle generated on } j \\ -1 & \text{if member has reverse oriented of the cycle generated on } j \\ 0 & \text{if member is not in the cycle whose generator is } j \end{cases}.$$

The matrices $\boldsymbol{B}_0$ and $\boldsymbol{B}_1$ depend on the shape of the structure and are not related to the cross-sectional area of the structure. Therefore, they are obtained only once in the analysis and do not need to be updated in each iteration step of the optimization.

For example, in the frame, in Fig. 7, the pattern of $\boldsymbol{B}_0$, $\boldsymbol{B}_1$ and $\boldsymbol{B}_1 \times \boldsymbol{B}_1'$ matrices are given in Fig. 8.

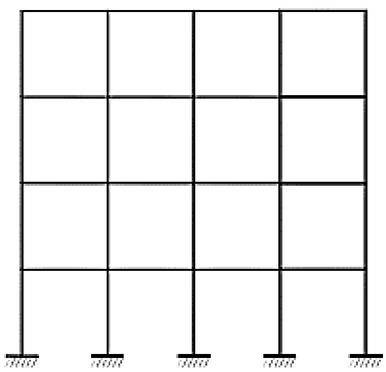

Fig. 7 A Simple planar frame S

3 Optimization algorithm

Metaheuristic algorithms are high-level search and optimization strategies inspired by natural, biological, and social processes. Unlike classical mathematical programming methods that often require gradient information or problem convexity, metaheuristics are derivative-free and capable of exploring large, complex, and multimodal search spaces. Their stochastic nature allows them to escape local optima and approximate near-global solutions with reasonable computational effort. In structural optimization, metaheuristics such as Genetic Algorithms (GA), Particle Swarm Optimization (PSO), Differential Evolution (DE), and more recently developed algorithms (e.g., Water Strider Algorithm, Whale Optimization Algorithm) have proven particularly effective in handling discrete design variables, nonlinear constraints, and large-scale design spaces. These methods balance exploration (global search) and exploitation (local refinement), making them highly suitable for practical engineering design problems where analytical solutions are intractable [23–25].

3.1 Water strider algorithm

Water striders are a fascinating group of insects known for their remarkable ability to navigate and stay above the water surface, which has captured human interest for many years [26, 27]. Their remarkable adaptation is attributed to their utilization of surface tension and hydrophobic properties, allowing them to remain buoyant on the water's surface. Additionally, their mechanisms of movement, communication, and behavioral patterns offer other intriguing characteristics that set them apart from other creatures [28].

Motivated by the unique features of these water-dwelling insects, the Water Strider Algorithm (WSA) has been

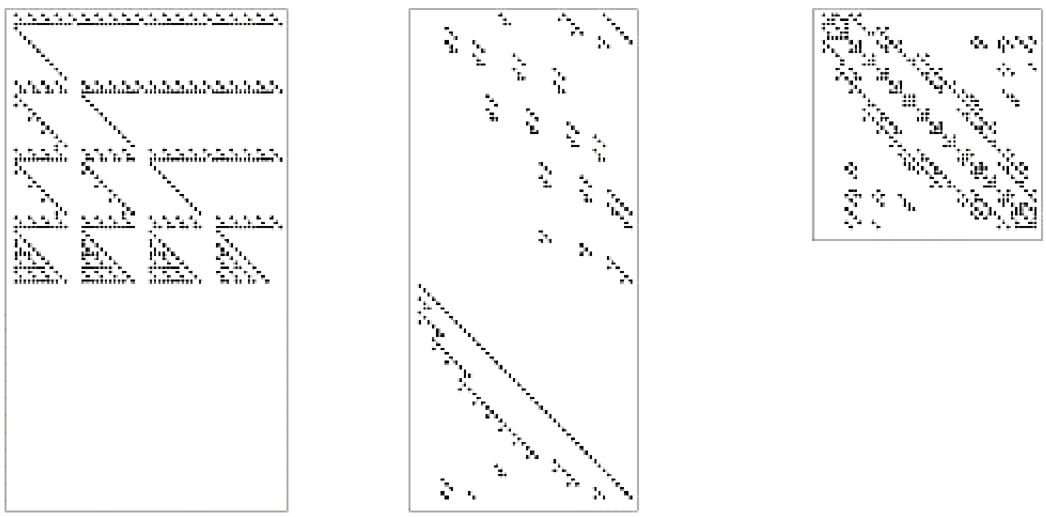

Fig. 8 Patterns of the $\boldsymbol{B}_0$, $\boldsymbol{B}_1$ and $\boldsymbol{B}_1^t\boldsymbol{B}_1$ matrices for S

developed. This algorithm draws inspiration from their efficient movement and behavior, translating these biological principles into computational methods for solving complex optimization problems.

The Water Strider Algorithm (WSA) is a bio-inspired optimization method that simulates the life cycle of water striders through five main stages: birth, territory establishment, mating, feeding, and death. In this framework, the search space is conceptualized as a lake containing multiple regions with potential solutions, while food represents the objective function to be optimized. Each stage plays a crucial role in guiding the optimization process: the birth stage generates new candidate solutions; in the territory establishment phase, solutions compete for dominance; the mating stage combines successful solutions to promote feature exchange; the feeding stage evaluates the solutions against the objective function; and finally, the death stage eliminates ineffective solutions, thereby ensuring a refined exploration of the search space [29–32].

In this study, WSA is employed as the optimization tool for the optimal design of frame structures. A population of N agents is initially generated randomly and evaluated with respect to the objective of minimizing structural weight. Agents are grouped into territories, where the best and worst individuals act as female and male representatives, respectively. Position updates are carried out through mating behaviors, attraction–repulsion mechanisms, and local foraging around promising regions. If a solution fails to improve, it is replaced by a newly initialized agent to maintain diversity within the population.

For the present work, the population size was set to 50, the maximum number of iterations to 400, and the stopping criterion was defined as either reaching this iteration limit or stagnation in fitness improvement. A penalty factor of 10^5 was used to handle design constraints. Parametric testing showed that increasing the population size enhances exploration but increases computational time, while smaller populations accelerate convergence at the expense of robustness. These details ensure the reproducibility of the proposed optimization procedure in the context of large-scale frame optimization. In addition to the common parameters (population size, maximum iterations, stopping criterion, and penalty factor), WSA also involves coefficients controlling the mating and attraction–repulsion processes, as well as the formation of territories. In this study, the default values suggested in the original literature were adopted, while sensitivity analyses were performed mainly on population size and iterations, since these parameters showed the greatest influence on computational performance.

To validate the effectiveness of WSA, a comparison was made with other widely used metaheuristic algorithms, the results of which are presented in Table 1 and Table 2 [29]. Summarize the performance of WSA against GA, PSO, and etc. on benchmark functions. The results indicate that WSA generally outperforms the other algorithms in terms of convergence speed, robustness, and final solution accuracy. This external evidence supports the suitability of WSA for large-scale structural optimization problems addressed in this study.

4 Optimization

Here it is desirable to minimize the weight of structural steel materials in the frames, subjected to compliance with the requirements of the design code. The objective function of the row is obtained by the following relation:

$$\text{Minimize } W(x) = \rho \sum_{i=1}^{Nd} A_i L_i \tag{5}$$

Table 1 The statistical results of unimodal benchmark functions 1–5

Function		WSA	GA	PSO	ICA	BBO	SSA	SCA
F1	Ave	1.09E-50	0.493651	474.0286	1.78E-27	0.631961	5.28E-09	1.94E-16
	Std	3.99E-50	0.976457	266.9246	4.27E-27	0.665318	8.26E-10	9.45E-16
F2	Ave	4.89E-28	0.027773	9.234122	4.24E-15	0.165913	0.535547	1.28E-18
	Std	1.94E-27	0.053506	2.396783	9.59E-15	0.057118	0.813057	4.59E-18
F3	Ave	0.014089	4682.494	4441.754	1.307412	10032.46	6.70E-07	650.4789
	Std	0.011180	1974.782	1762.155	0.812703	3031.347	4.49E-07	1248.101
F4	Ave	0.000490	9.282368	14.10854	0.069323	7.924755	1.328179	1.335270
	Std	0.000354	2.208485	2.390036	0.093936	1.155925	1.611482	1.828663
F5	Ave	32.42146	481.1478	31370.23	107.5567	219.3536	67.11092	27.51712
	Std	29.52849	481.3205	24726.88	135.2055	151.6324	84.22198	0.556120

Table 2 The unimodal benchmark functions

Function	Dim	Range	f_{min}
$F_1(x)=\sum_{i=1}^{n} x_i^2$	30	[−100,100]	0
$F_2(x)=\sum_{i=1}^{n} \lvert x_i \rvert + \prod_{i=1}^{n} \lvert x_i \rvert$	30	[−10,10]	0
$F_3(x)=\sum_{i=1}^{n}\left(\sum_{j-1}^{i} x_i^2\right)^2$	30	[−100,100]	0
$F_4(x)=\max_i \{\lvert x_i \rvert, 1 \le i \le n\}$	30	[−100,100]	0
$F_5(x)=\sum_{i=1}^{n}\left[100\left(x_{i+1}-x_i^2\right)^2+\left(x_i-1\right)^2\right]$	30	[−30,30]	0

$$\text{Subject to } g_j(x) \le 0 \tag{6}$$

where ρ is the unit weight of the steel volume, A is the cross-sectional area and L is the length of the member.

The functions $g(x)$ of stress and displacement limits are defined as

$$g_\sigma^k(x)=\frac{\sigma_k}{(\sigma_k)_{\text{allowable}}}-1 \le 0 \quad k=1,2,\ldots,N_d \tag{7}$$

$$g_d^n(x)=\frac{d_n}{(d_n)_{\text{allowable}}}-1 \le 0 \quad n=1,2,\ldots,N_n \tag{8}$$

$$g_\lambda^k(x)=\frac{\lambda_k}{(\lambda_k)_{\text{allowable}}}-1 \le 0 \quad k=1,2,\ldots,N_d \tag{9}$$

where σ is the stress of the members, d the displacement of the nodes, N_n the number of nodes and λ the slenderness of the members.

To implement the WSA meta-heuristic algorithm, the following function is considered to apply the penalty coefficient, where K_p is the penalty coefficient and W is the initial raw weight function [18]:

$$\text{Minimize } q(x)=w\left(1+K_p\sum\max\left(g(x),0\right)\right). \tag{10}$$

5 Examples

This section presents the analysis and design of three specialized high-rise frames utilizing both the force and displacement methods. Notably, these examples exhibit a lower DSI compared to the DKI, and the results demonstrate significant reductions in analysis time and memory usage when applying the force method.

5.1 Example 1: A 189-members frame

The 189-member frame, illustrated in Fig. 9, comprises a total of 112 nodes, with an elastic modulus of 210 GPa.

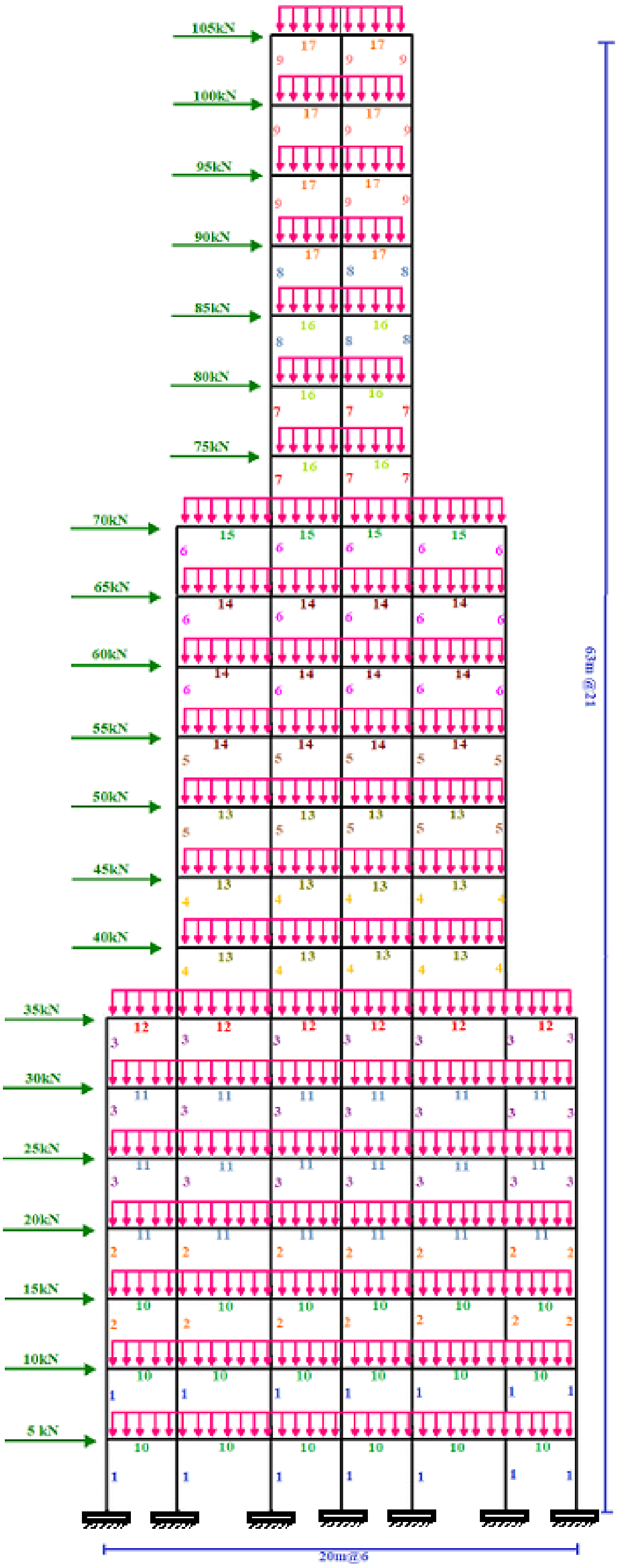

Fig. 9 Geometry and the member grouping of the 189-member frame

The members of this frame are categorized into 17 distinct groups. DSI is recorded as 255, while DKI is 312. The dimensions of the $\boldsymbol{B}_1$ matrix are 1134 × 504, and the dimensions of the $\boldsymbol{B}_0$ matrix are similarly 1134 × 630.

Table 3 provides a comprehensive list of the available sections for this frame. Additionally, Fig. 10 shows the structure of the $\boldsymbol{B}_1 \times \boldsymbol{B}_1'$ matrix, which measures 1134 × 1134, containing 9760 non-zero entries, while the $\boldsymbol{B}_1$ matrix itself has 2314 non-zero entries.

Using the Water Strider Algorithm (WSA), optimization was conducted for both the force and displacement methods, yielding comparable results as anticipated. The convergence diagrams for these optimization processes are presented in Fig. 11, alongside the optimal list of sections and results in Table 4 specific to the 189-member frame.

Furthermore, a comparison of the computational time required for optimization using both the force and displacement methods is illustrated in Fig. 12. The results clearly indicate that the optimization time for the force method is

Table 3 List of the available sections for the frame's models

Section ID	Section name	Area (10^{-4} m^2)	Section ID	Section name	Area (10^{-4} m^2)
1	W6X9	17.29	29	W12X40	76.13
2	W8X10	19.1	30	W18X40	76.13
3	W10X12	22.84	31	W8X48	90.97
4	W6X12	22.9	32	W21X50	94.84
5	W4X13	24.71	33	W12X53	100.64
6	W8X13	24.77	34	W18X55	104.52
7	W12X14	26.84	35	W24X68	129.68
8	W10X15	28.45	36	W18X76	143.87
9	W6X15	28.58	37	W27X94	178.71
10	W5X16	30.19	38	W24X104	197.42
11	W12X16	30.39	39	W27X114	216.13
12	W10X17	32.19	40	W27X129	243.87
13	W8X18	33.94	41	W33X141	268.39
14	W5X19	35.74	42	W24X146	277.42
15	W12X19	35.94	43	W21X147	278.71
16	W10X19	36.26	44	W14X159	301.29
17	W8X21	39.74	45	W27X178	337.42
18	W14X22	41.87	46	W40X192	364.52
19	W10X26	49.1	47	W44X198	374.19
20	W12X26	49.35	48	W12X210	398.71
21	W16X26	49.55	49	W24X229	433.55
22	W14X26	49.61	50	W33X241	457.42
23	W12X30	56.71	51	W40X277	524.52
24	W16X31	58.84	52	W36X328	621.93
25	W10X33	62.65	53	W27X368	696.77
26	W12X35	66.45	54	W40X480	903.22
27	W18X35	66.45	55	W36X588	1109.68
28	W16X36	68.39	56	W14X605	1148.38

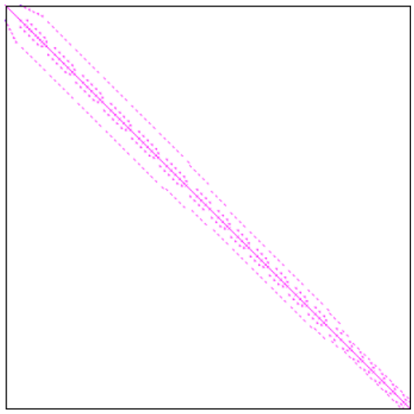

Fig. 10 Pattern of the $\boldsymbol{B}_1 \times \boldsymbol{B}_1'$ matrix for the 189-member frame with 9760 non-zero entries

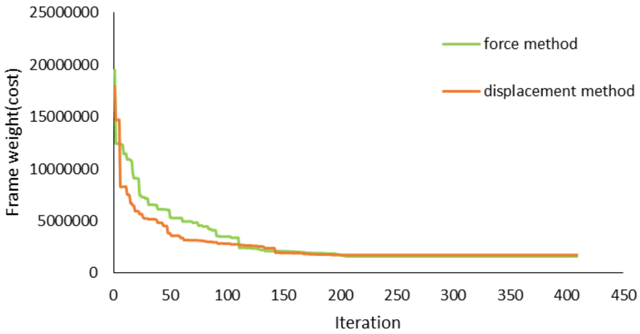

Fig. 11 Convergence curves for optimization of the 189-member frame

Table 4 Results of the optimization for the 189-member frame

Group No. of elements	Displacement method section No.	Force method section No.
1	3	3
2	2	11
3	8	1
4	44	1
5	3	4
6	3	10
7	7	13
8	9	5
9	1	8
10	2	7
11	16	15
12	3	18
13	24	27
14	1	12
15	32	22
16	7	11
17	26	3
Best cost (kg)	1747788	1713700
Average (kg)	1805423	1789220
Std	546289	491974

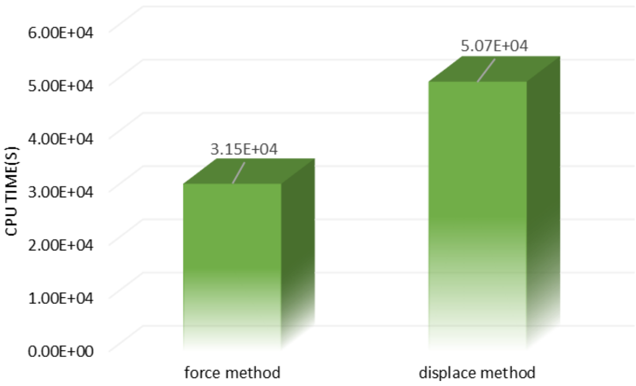

Fig. 12 Comparison of the time for optimization using force method and displacement approach for the 189-member frame

considerably less than that required by the displacement approach, highlighting the efficiency advantages gained by utilizing the force method in the analysis of the frame.

5.2 Example 2: A 251-member frame

The second example in this study features a hexa-gride frame consisting of 5 bays and 21 stories, as depicted in Fig. 13. The elements of this frame are organized into 17 distinct groups. The design variables for the frame components have been selected from a range of 55 W-sections. The yield stress of the members is set at 2400 kPa, and the elastic modulus is specified as 210 GPa. Strength and displacement constraints are applied in accordance with the AISC-LRFD standards.

The degree of statical indeterminacy for this structure is 483, while the degree of kinematical indeterminacy is 669. Given these values, it is anticipated that the force method will demonstrate greater efficiency in terms of computation time when compared to the displacement method.

The dimensions of the $\boldsymbol{B}_1$ matrix are 1506 × 636, and the dimensions of the $\boldsymbol{B}_0$ matrix are also 1506 × 876. Fig. 14 illustrates the structure of the $\boldsymbol{B}_1 \times \boldsymbol{B}_1'$ matrix, which measures 1506 × 1506 and contains 12,866 non-zero entries. The $\boldsymbol{B}_1$ matrix itself features 5,840 non-zero entries.

Optimization was performed using the Water Strider Algorithm (WSA) for the analysis of the frame, applying both the force and displacement methods. As expected, the results obtained from these two methods were similar. The convergence diagrams illustrating the responses are shown in Fig. 15, while Table 5 presents the optimal section lists and results specific to the 251-member frame.

A comparison of the optimization times for the force and displacement methods is depicted in Fig. 16. The results indicate that the optimization time required for the force method is significantly less than that for the displacement

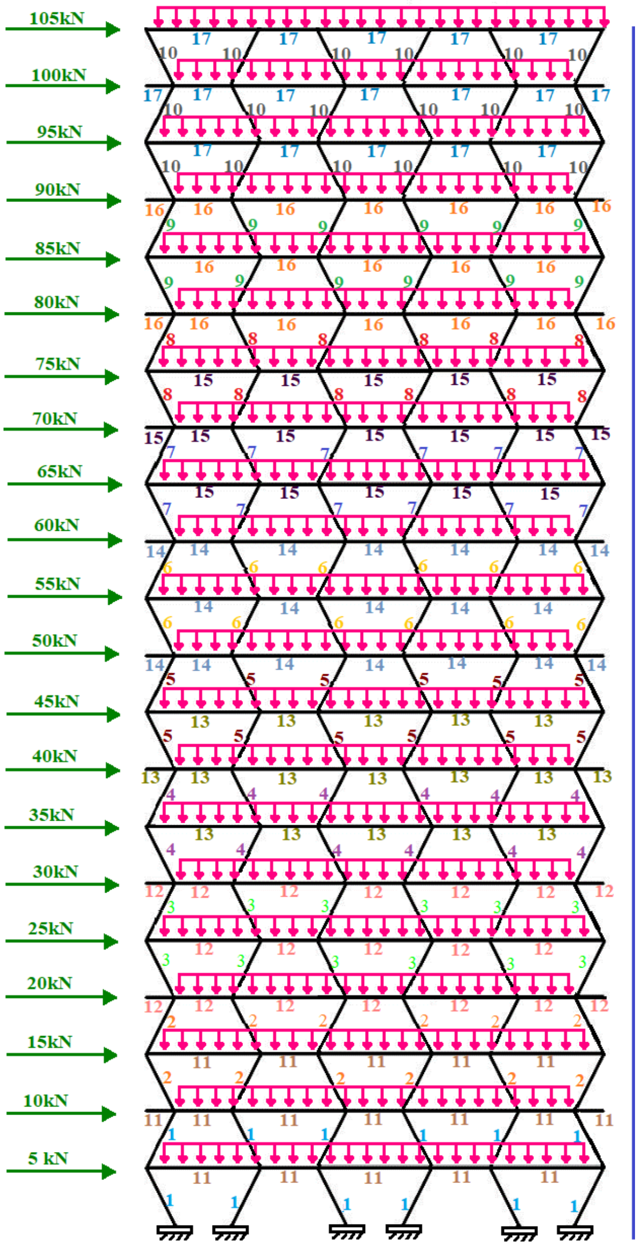

Fig. 13 Geometry and the member grouping of the 251-member frame

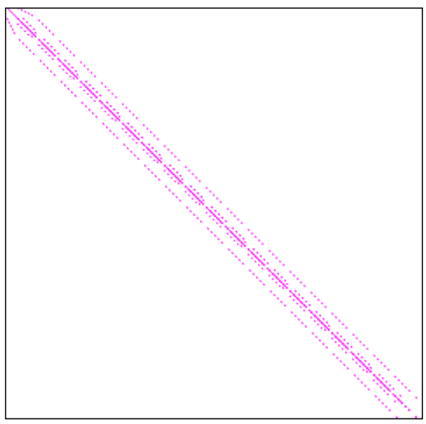

Fig. 14 Pattern of the $\boldsymbol{B}_1 \times \boldsymbol{B}_1'$ matrix for the 251-member frame with 12866 non-zero entries

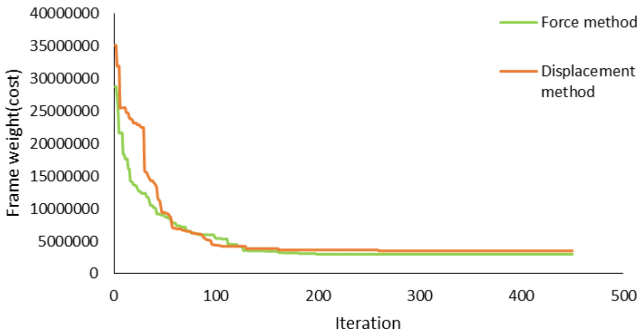

Fig. 15 Convergence curves for optimization of the 251-member frame

Table 5 Results of the optimization for the 251-member frame

Group No. of elements	Displacement method section No.	Force method section No.
1	8	4
2	11	10
3	18	22
4	3	21
5	28	12
6	17	11
7	13	11
8	3	4
9	1	1
10	1	1
11	13	17
12	1	2
13	2	3
14	18	15
15	10	9
16	4	3
17	7	6
Best cost (kg)	3523200	2998700
Average (kg)	3248912	2258630
Std	742537	701856

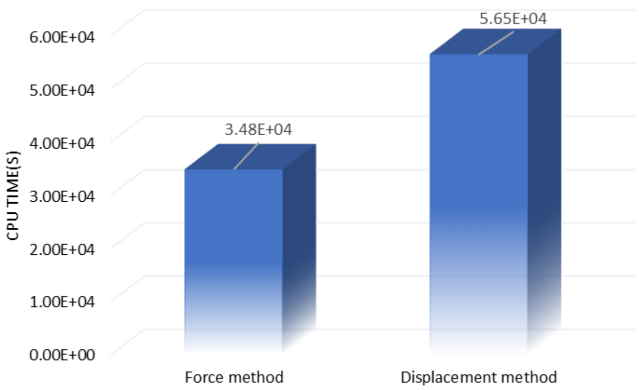

Fig. 16 Comparison of the time for optimization using force method and displacement approach for the 251-member frame

method, reaffirming the efficiency advantages of the force method in this example.

5.3 Example 3: A 292-member frame

The third example features a frame composed of 292 members, as illustrated in Fig. 17. This frame contains a total of 164 nodes, with an elastic modulus of 210 GPa. The members are classified into 26 distinct groups. For this frame, DSI is recorded as 411, and the DKI is 465.

The dimensions of the $\boldsymbol{B}_1$ matrix are 1752 × 816, while the dimensions of the $\boldsymbol{B}_0$ matrix are similarly 1752 × 936. Table 3 provides a list of the available sections for this frame. Fig. 18 displays the structure of the $\boldsymbol{B}_1 \times \boldsymbol{B}_1'$ matrix, which measures 1752 × 1752, containing 10,804 non-zero entries. The $\boldsymbol{B}_1$ matrix itself has 2,582 non-zero entries.

Using the Water Strider Algorithm (WSA), optimization was carried out for the analysis of the frame with both force and displacement methods. As anticipated, the results obtained from these methods were comparable. The convergence diagrams illustrating the responses are shown in Fig. 19, and the optimum list of sections along with the results are presented in Table 6 for the 292-member frame.

Finally, the comparison of optimization times for the force and displacement methods is depicted in Fig. 20. The findings indicate that the optimization time required for the force method is significantly less than that for the displacement method, further confirming the efficiency of the force method in structural analysis and optimization tasks.

6 Limitations and counterexamples

In addition to the large-scale cases with DSI < DKI, we included a counterexample where DKI < DSI (two-bay, one-story frame with added braces: DSI = 12, DKI = 9). Under identical WSA settings (population = 50, max iterations = 400, penalty = 10^5), the displacement method required smaller linear systems (9 × 9 vs. 12 × 12) and achieved a ~33% lower CPU time (1.08 s vs. 1.62 s), while yielding a similar optimal weight (102.7 vs. 102.8 kN). This demonstrates that the advantage of the force method is not universal and depends on the DSI/DKI relationship. Fig. 21 shows a simple frame with DKI < DSI. The comparison results are shown in Table 7.

The idea of this paper can be extended to other optimization problems such as those in [33, 34].

Fig. 17 Geometry and the member grouping of the 292-member frame

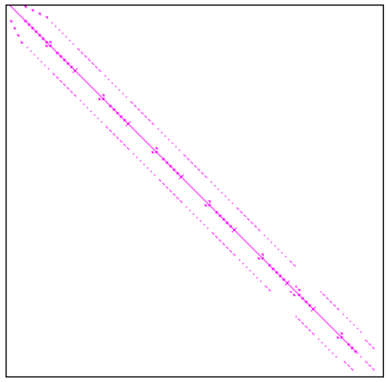

Fig. 18 Pattern of the $\boldsymbol{B}_1 \times \boldsymbol{B}_1'$ matrix for the 292-member frame with 10804 non-zero entries

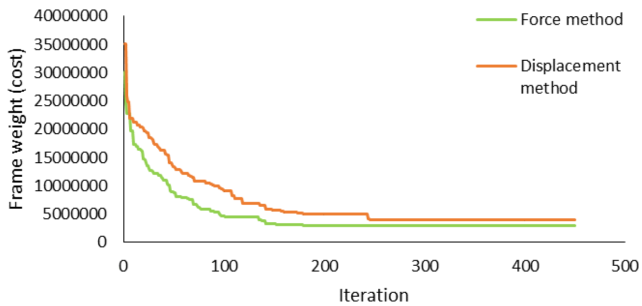

Fig. 19 Convergence curves for optimization of the 292-member frame

7 Conclusions

The primary objective of this article is to compare two structural analysis methods for specialized tall frames: the force method and the displacement method. In this study, the force method is implemented using graph theory principles. The design seeks to minimize the weight of the structure while adhering to the LRFD (Load and Resistance Factor Design) limits for the frames. To achieve this optimization, the Water Strider Algorithm (WSA) was utilized to manage the segment indicators as discrete design variables.

The present study introduces the Water Strider Algorithm (WSA) as a novel optimizer and applies it to large-scale, highly indeterminate frame structures. Unlike earlier works that mainly focused on improving existing algorithms such as PSO-SRM and validating the method on benchmark examples, this study demonstrates that WSA can achieve competitive performance while significantly reducing computational time in complex high-rise frames. The results confirm that the advantages of the force method over the displacement method become more pronounced in large-scale problems with DSI < DKI. Therefore, the contributions of this work are twofold:

1. the integration of a new bio-inspired algorithm (WSA) into the force method framework, and
2. the demonstration of scalability and efficiency in the optimal design of real-world large frame structures.

Table 6 Results of the optimization for the 292-member frame

Group No. of elements	Displacement method section No.	Force method section No.
1	1	1
2	2	4
3	18	3
4	11	1
5	14	8
6	18	7
7	24	4
8	5	10
9	19	3
10	30	48
11	28	5
12	23	2
13	43	12
14	29	25
15	29	6
16	20	3
17	16	8
18	4	26
19	33	21
20	7	5
21	25	12
22	19	22
23	34	4
24	37	36
25	48	7
26	31	17
Best cost (kg)	3940365	2863200
Average (kg)	3524195	2548930
Std	86254	54789

The optimal weight values obtained for all three frames were found to be comparable between the two methods. However, a significant finding is the comparison of CPU time required for each analytical method. In all three cases, the CPU time for the force method was consistently lower than that of the displacement approach. Furthermore, as the differences in DSI (Degree of Static Indeterminacy) and DKI (Degree of Kinematic Indeterminacy) increased, the distinction in CPU time between the two methods also grew more pronounced. These findings are illustrated in Fig. 22, providing a visual representation of the comparative results.

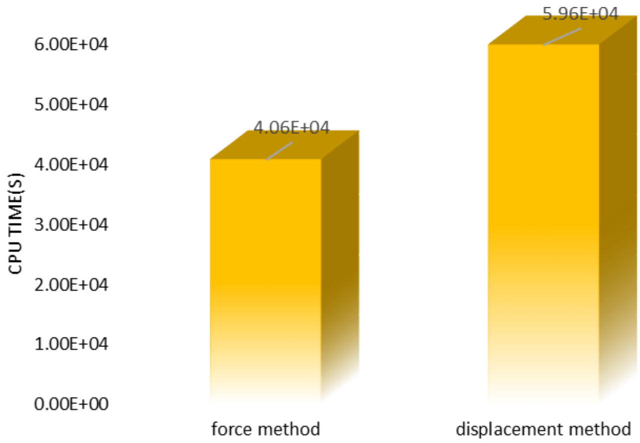

Fig. 20 Comparison of the time for optimization using force method and displacement method for the 292-member frame

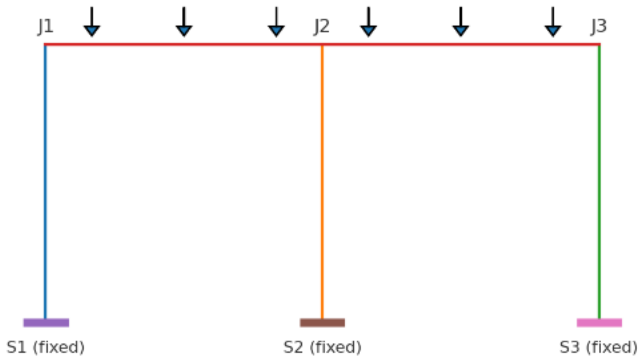

Fig. 21 Counterexample frame (two-bay, one-story) with DKI < DSI

Table 7 Performance comparison for the counterexample (DKI < DSI)

Metric	Force method	Displacement method
DSI/DKI	12/9	12/9
Avg. linear system size per fitness eval	12 × 12	9 × 9
WSA fitness evaluations	20,000	20,000
CPU time [s]	1.62	1.08
Final optimal weight [kN]	102.8	102.7
Convergence iterations to ±0.1%	389	340

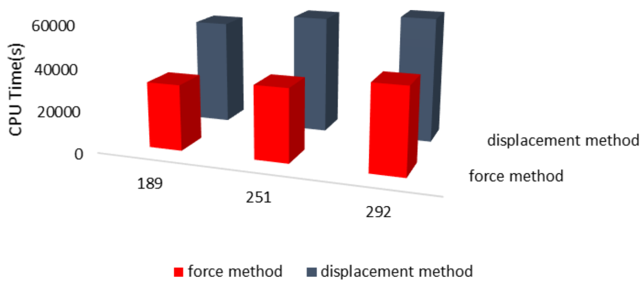

Fig. 22 Comparison of optimization time in the force method and the displacement method for three frames

References

[1] Kaveh, A. "Structural Mechanics: Graph and Matrix Methods", Research Studies Press Ltd., 2004. ISBN 978-0863803048

[2] Kaveh, A. "Optimal Structural Analysis", John Wiley & Sons, 2006. ISBN 9780470030158
https://doi.org/10.1002/9780470033326

[3] Kaveh, A., Zaerreza, A. "Comparison of the graph-theoretical force method and displacement method for optimal design of frame structures", Structures, 43, pp. 1145–1159, 2022. https://doi.org/10.1016/j.istruc.2022.07.035

[4] Argyris, J. H., Kelsey, S. "Energy Theorems and Structural Analysis: A Generalised Discourse with Applications on Energy Principles of Structural Analysis Including the Effects of Temperature and Non-Linear Stress-Strain Relations", Springer, 1960. ISBN 978-1-4899-5852-5 https://doi.org/10.1007/978-1-4899-5850-1

[5] Kaveh, A. "Recent developments in the force method of structural analysis", Applied Mechanics Reviews, 45(9), pp. 401–418, 1992. https://doi.org/10.1115/1.3119768

[6] de C. Henderson, J. C. "Topological Aspects of Structural Analysis: Improving the Conditioning of the Equations of Compatibility of a Multi-Member Skeletal Structure by Use of the Knowledge of Topology", Aircraft Engineering, 32(5), pp. 137–141, 1960. https://doi.org/10.1108/eb033249

[7] Maunder, E. A. W. "Topological and linear analysis of skeletal structures", PhD Thesis, University of London, 1971.

[8] de Henderson, J. C. C., Maunder, E. A. W. "A Problem in Applied Topology: on the Selection of Cycles for the Flexibility Analysis of Skeletal Structures", IMA Journal of Applied Mathematics, 5(2), pp. 254–269, 1969. https://doi.org/10.1093/imamat/5.2.254

[9] Denke, P. H. "A general digital computer analysis of statically indeterminate structures", National Aeronautics and Space Administration, Washington, DC, USA, NASA TN D-1666, 1962.

[10] Robinson, J., Haggenmacher, G. "Some new developments in matrix force analysis", In: Gallagher, R. H., Yamada, Y., Oden, J. T. (eds.) Recent Advances in Matrix Methods of Structural Analysis and Design, University of Alabama Press, 1971, pp. 183–228. ISBN 9780817335052

[11] Topcu, A. "A contribution to the systematic analysis of finite element structures using the force method", Doctoral Dissertation, University of Essen, 1979.

[12] Kaneko, I., Lawo, M., Thierauf, G. "On computational procedures for the force method", International Journal for Numerical Methods in Engineering, 18(10), pp. 1469–1495, 1982. https://doi.org/10.1002/nme.1620181004

[13] Soyer, E., Topcu, A. "Sparse self-stress matrices for the finite element force method", International Journal for Numerical Methods in Engineering, 50(9), pp. 2175–2194, 2001. https://doi.org/10.1002/nme.119

[14] Kaveh, A. "The application of topology and matroid theory to the analysis of structures", PhD Thesis, University of London, 1974.

[15] Kaveh, A. "Improved cycle bases for the flexibility analysis of structures", Computer Methods in Applied Mechanics and Engineering, 9(3), pp. 267–272, 1976. https://doi.org/10.1016/0045-7825(76)90031-1

[16] Kaveh, A. "Topological transformations for efficient structural analysis", Springer, 2022. ISBN 978-3-031-12299-6 https://doi.org/10.1007/978-3-031-12300-9

[17] Cassell, A. C. "An alternative method for finite element analysis; A combinatorial approach to the flexibility method for structural continua and to analogous methods in field analysis", Proceedings of the Royal Society of London. A. Mathematical and Physical Sciences, 352(1668), pp. 73–89, 1976. https://doi.org/10.1098/rspa.1976.0164

[18] Kaveh, A., Khavaninzadeh, N. "Optimal Design of Planar Trusses Using Graph Theoretical Force Method", Periodica Polytechnica Civil Engineering, 67(2), pp. 337–348, 2023. https://doi.org/10.3311/PPci.21410

[19] Kaveh, A., Rahami, H. "Analysis, design and optimization of structures using force method and genetic algorithm", International Journal for Numerical Methods in Engineering, 65(10), pp. 1570–1584, 2006. https://doi.org/10.1002/nme.1506

[20] Kaveh, A., Malakouti Rad, S. "Hybrid Genetic Algorithm and Particle Swarm Optimization for the Force Method-based Simultaneous Analysis and Design", Iranian Journal of Science and Technology, Transaction B: Engineering, 34(B1), pp. 15–34, 2010.

[21] Kaveh, A., Massoudi, M. S., Massoudi, M. J. "Efficient finite element analysis using graph-theoretical force method; rectangular plane stress and plane strain serendipity family elements", Periodica Polytechnica Civil Engineering, 58(1), pp. 3–22, 2014. https://doi.org/10.3311/PPci.7405

[22] Kaveh, A. "A combinatorial optimization problem; optimal generalized cycle bases", Computer Methods in Applied Mechanics and Engineering, 20(1), pp. 39–52, 1979. https://doi.org/10.1016/0045-7825(79)90057-4

[23] Lagaros, N. D., Plevris, V., Kallioras, N. A. "The Mosaic of Metaheuristic Algorithms in Structural Optimization", Archives of Computational Methods in Engineering, 29(7), pp. 5457–5492, 2022. https://doi.org/10.1007/s11831-022-09773-0

[24] Ghaemifard, S., Ghannadiasl, A. "A Comparison of Metaheuristic Algorithms for Structural Optimization: Performance and Efficiency Analysis", Advances in Civil Engineering, 2024(1), 2054173, 2024. https://doi.org/10.1155/2024/2054173

[25] Houssein, E. H., Saeed, M. K., Hu, G., Al-Sayed, M. M. "Metaheuristics for Solving Global and Engineering Optimization Problems: Review, Applications, Open Issues and Challenges", Archives of Computational Methods in Engineering, 31(8), pp. 4485–4519, 2024. https://doi.org/10.1007/s11831-024-10168-6

[26] Zhang, X., Zhao, J., Zhu, Q., Chen, N., Zhang, M., Pan, Q. "Bioinspired aquatic microrobot capable of walking on water surface like a water strider", ACS Applied Materials & Interfaces, 3(7), pp. 2630–2636, 2011. https://doi.org/10.1021/am200382g

[27] Wei, P. J., Chen, S. C., Lin, J. F. "Adhesion forces and contact angles of water strider legs", Langmuir, 25(3), pp. 1526–1528, 2009. https://doi.org/10.1021/la803223r

[28] Hu, D. L., Bush, J. W. M. "The hydrodynamics of water-walking arthropods", Journal of Fluid Mechanics, 644, pp. 5–33, 2010. https://doi.org/10.1017/S0022112009992205

[29] Kaveh, A., Dadras Eslamlou, A. "Water strider algorithm: A new metaheuristic and applications", Structures, 25, pp. 520–541, 2020. https://doi.org/10.1016/j.istruc.2020.03.033

[30] Bruggi, M., Ismail, H., Lógó, J. "Topology optimization with graded infill accounting for loading uncertainty", Composite Structures, 311, 116807, 2023. https://doi.org/10.1016/j.compstruct.2023.116807

[31] Lógó, J., Ghaemi, M., Movahedi Rad, M. "Optimal topologies in case of probabilistic loading: the influence of load correlation", Mechanics Based Design of Structures and Machines, 37(3), pp. 327–348, 2009. https://doi.org/10.1080/15397730902936328

[32] Movahedi Rad, M., Habashneh, M., Lógó, J. "Elasto-plastic limit analysis of reliability based geometrically nonlinear bi-directional evolutionary topology optimization", Structures, 34, pp. 1720–1733, 2021. https://doi.org/10.1016/j.istruc.2021.08.105

[33] Movahedi Rad, M., Khaleel Ibrahim, S. "Optimal Plastic Analysis and Design of Pile Foundations Under Reliable Conditions", Periodica Polytechnica Civil Engineering, 65(3), pp. 761–767, 2021. https://doi.org/10.3311/PPci.17402

[34] Habashneh, M., Movahedi Rad, M. "Optimizing structural topology design through consideration of fatigue crack propagation", Computer Methods in Applied Mechanics and Engineering, 419, 116629, 2024. https://doi.org/10.1016/j.cma.2023.116629